Angewandte
Eine Zeitschrift der Gesellschaft Deutscher Chemiker
Chemie

Supporting Information

Structural and Spectroscopic Characterization of a High-Spin {FeNO}^{6} Complex with an Iron(IV)–NO$^-$ Electronic Structure

*Amy L. Speelman, Bo Zhang, Carsten Krebs, and Nicolai Lehnert**

ange_201601742_sm_miscellaneous_information.pdf

Table of Contents

Synthetic Procedures

Preparation and handling of air sensitive materials was carried out under a dinitrogen atmosphere in an MBraun glovebox equipped with a circulating purifier (O_2, $H_2O < 0.1$ ppm) or by using standard Schlenk techniques. Solvents and reagents were purchased and used as supplied except as follows. Acetonitrile, deuterated acetonitrile, propionitrile, and butyronitrile were distilled from calcium hydride, and diethyl ether was distilled from sodium benzophenone. All solvents were freeze-pump-thawed to remove dioxygen and stored over molecular sieves. Nitric oxide (Cryogenic Gases Inc., 99.5%) was purified by passage through an ascarite II column (NaOH on silica) followed by a cold trap at -80°C in order to remove higher nitrogen oxide impurities. Nitric oxide-$^{15}N^{18}O$ (Sigma-Aldrich) was used without further purification. Tetrabutylammonium hexafluorophosphate was recrystallized from ethanol. Thianthrene tetrafluoroborate was prepared by oxidation of thianthrene with nitrosonium tetrafluoroborate following a literature procedure.[1] $[Fe(TMG_3tren)(NO)](OTf)_2$ was prepared as previously described.[2] $Fe(CH_3CN)_6(BF_4)_2$ was synthesized by oxidation of iron powder with nitrosonium tetrafluoroborate following a literature procedure.[3] $[Fe(TMG_3tren)(NO)](BF_4)_2$ was synthesized by metalation of the TMG_3tren ligand with $Fe(CH_3CN)_6(BF4)_2$ followed by exposure to excess NO gas in a manner analogous to the triflate complex.[2] ^{57}Fe complexes (with tetrafluoroborate counterions) were synthesized in a manner analogous to the natural abundance complexes. The solution of the $\{^{57}FeNO\}^8$ complex used for Mössbauer spectroscopy was generated by reduction of the corresponding $\{^{57}FeNO\}^7$ complex with 1.2 equivalents of bis(pentamethylcyclopentadienyl)cobalt(II) as previously described.[2]

The $\{FeNO\}^6$ complex $[Fe(TMG_3tren)(NO)]^{3+}$ (**1**) was prepared by addition of a slight excess (1.2-1.5 equivalents) of thianthrene tetrafluoroborate to $[Fe(TMG_3tren)(NO)](X)_2$ (**2**; X = OTf or BF_4), typically in the 5-15 mM concentration range with respect to Fe, in CH_3CN. The $\{FeNO\}^6$ complex can be precipitated by addition of diethyl ether to these solutions (Fig. S4), but since precipitation generally leads to partial decomposition, all characterization was carried out on freshly prepared solutions of the complex. EPR (Figure S3), solution IR (Figure S2), and/or NMR (Figure S5) spectroscopy were used to confirm sample purity. The $\{^{57}FeNO\}^6$ solution used for Mössbauer spectroscopy was prepared in a manner analogous to the unlabeled compound.

Physical measurements

Infrared spectra of solid samples were obtained from KBr disks on Perkin-Elmer BX, GX, or RX1 spectrometers, and the IR spectra of solution samples were obtained in cells equipped with CaF_2 windows on the same instruments. Proton NMR spectra were recorded on a Varian MR 400 MHz instrument or a Varian VNMRS 500 MHz instrument. Solution magnetic susceptibility measurements were performed on

[1] B. Boduszek, H. J. Shine, *J. Org. Chem.* **1988**, *53*, 5142-5143.
[2] A. L. Speelman, N. Lehnert, *Angew. Chem.* **2013**, *125*, 12509-12513; *Angew. Chem. Int. Ed.* **2013**, *52*, 12283-12287.
[3] a) R. A. Heintz, J. A. Smith, P. S. Szalay, A. Weisgerber, K. R. Dunbar, in *Inorganic Syntheses, Vol. 33* (Ed.: D. Coucouvanis), John Wiley & Sons, Inc., **2002**, pp. 75-121. b) B. J. Hathaway, D. G. Holah, A. E. Underhill, *J. Chem. Soc.* **1962**, 2444-2448. c) B. J. Hathaway, A. E. Underhill, *J. Chem. Soc.* **1960**, 3705-3711.

a Varian MR 400 MHz instrument at 295 K using the Evans method.[4] Diamagnetic corrections were determined from Pascal's constants. Electronic absorption spectra were recorded using an Analytical Jena Specord S600 instrument. Electron paramagnetic resonance spectra were measured on a Bruker X-Band EMX spectrometer equipped with an Oxford Instruments liquid helium cryostat. Cyclic voltammograms were obtained using a CH instruments CHI600E electrochemical workstation using a three component system consisting of a glassy carbon working electrode, a platinum counter electrode, and a silver wire pseudo-reference electrode. Potentials were corrected to Fc/Fc^{+} using an internal ferrocene standard. UV-Visible and IR spectroelectrochemistry experiments were performed using custom-built thin layer electrochemical cells as previously described.[5] All electrochemical and spectroelectrochemical measurements were performed in the presence of 0.1 M tetrabutylammonium hexafluorophosphate or 0.1 M tetrabutylammonium perchlorate as supporting electrolyte.

Mössbauer spectra were recorded on spectrometers from SEECO (Edina, MN). The spectrometer used to record the weak-field spectra is equipped with a Janis SVT-400 variable-temperature cryostat, whereas the spectrometer used to acquire the strong-field spectra is equipped with a Janis 8TMOSS-OM-12SVT variable-temperature cryostat. The quoted isomer shifts are relative to the centroid of the spectrum of α-iron metal at room temperature. Simulations of the Mössbauer spectra were carried out using the WMOSS spectral analysis software from SEECO (www.wmoss.org; Edina, MN). Some of the simulations are based on the commonly used spin Hamiltonian (Equation 1) in which the first three terms describe the electron Zeeman effect and zero field splitting (ZFS) of the electron spin ground state, the fourth term represents the interaction between the electric field gradient and the nuclear quadrupole moment, the fifth term describes the magnetic hyperfine interactions of the electronic spin with the ^{57}Fe nucleus, and the last term represents the ^{57}Fe nuclear Zeeman interaction.

$$\begin{aligned}\mathbf{H} = \beta \mathbf{S} \bullet \mathbf{g} \bullet \mathbf{B} + D\left(\mathbf{S}_{\mathbf{z}}^2 - \frac{S(S+1)}{3}\right) + E\left(\mathbf{S}_{\mathbf{x}}^2 - \mathbf{S}_{\mathbf{y}}^2\right) \\ + \frac{\mathbf{eQV_{zz}}}{4}\left[\mathbf{I}_{\mathbf{z}}^2 - \frac{I(I+1)}{3} + \frac{\eta}{3}\left(\mathbf{I}_{\mathbf{x}}^2 - \mathbf{I}_{\mathbf{y}}^2\right)\right] + \mathbf{S} \bullet \mathbf{A} \bullet \mathbf{I} - g_n \beta_{\mathbf{n}} \mathbf{B} \bullet \mathbf{I}\end{aligned} \quad (1)$$

All simulations were carried out in the slow relaxation regime.

[4] a) D.F. Evans *J. Chem. Soc.* **1959**, 2003-2005. b) E.M. Schubert *J. Chem. Ed.* **1992**, *69*, 62. c) G.A. Bain, J.F Berry *J. Chem. Ed.* **2008**, *85*, 532-536.
[5] L. E. Goodrich, S. Roy, E. E. Alp, J. Zhao, M. Y. Hu, N. Lehnert, *Inorg. Chem.* **2013**, *52*, 7766-7780

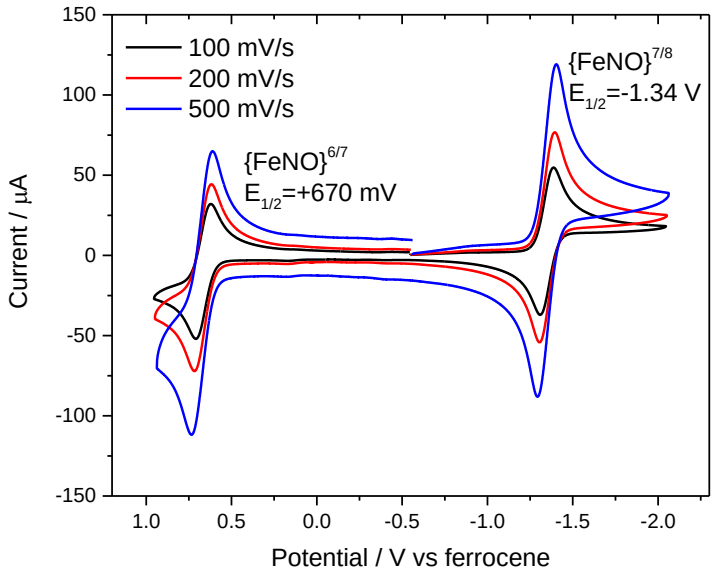

Figure S1. Cyclic voltammogram of [Fe(TMG$_3$tren)(NO)](OTf)$_2$ (**2**) at variable scan rates in CH_3CN.

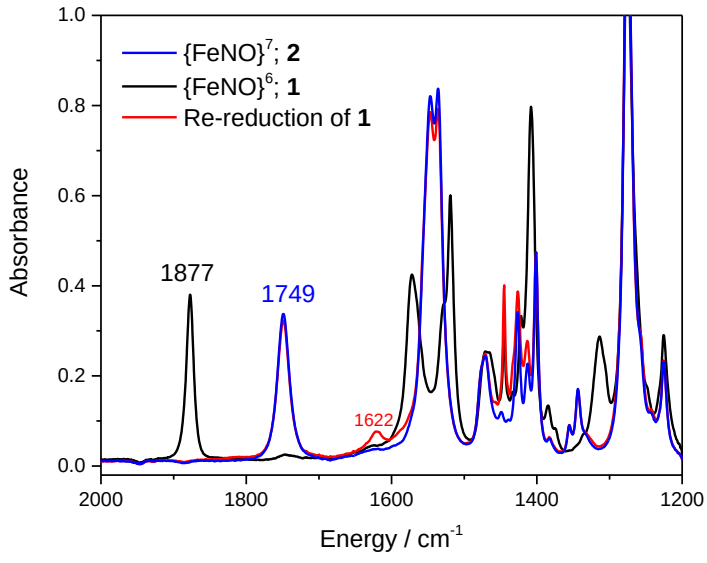

Figure S2. Solution IR showing the oxidation of [Fe(TMG$_3$tren)(NO)][(OTf)$_2$ (**2**) to the corresponding {FeNO}^{6} complex (**1**) using excess (1.3 equivalents) thianthrene tetrafluoroborate ($E_{1/2}$ = +860 mV vs ferrocene) in CD_3CN at room temperature. The oxidation is almost fully reversible upon addition of ferrocene. The peak at 1622 cm^{-1} in the re-reduced complex is the result of formation of a minor ferric impurity.

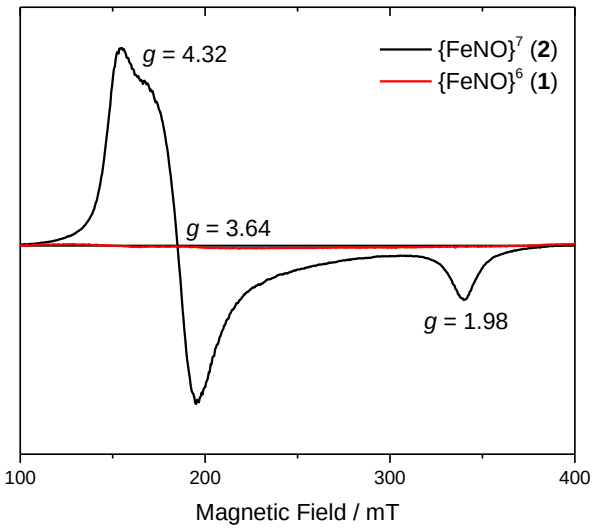

Figure S3. EPR spectra of frozen acetonitrile solutions (5 mM) showing the clean conversion of the *S* = 3/2{FeNO}^{7} complex (**2**) to the corresponding EPR-silent {FeNO}^{6} complex (**1**) upon addition of thianthrene tetrafluoroborate. Conditions: Temperature = 4.2 K; Frequency = 9.351 GHz; Microwave power = 20.5 mW; Modulation frequency = 100 kHz; Modulation amplitude = 1 G. The spectrum of **2** dissolved in acetonitrile is broader than that of **2** dissolved in CH_2Cl_2[2], suggesting that **2** exhibits greater conformational heterogeneity in acetonitrile.

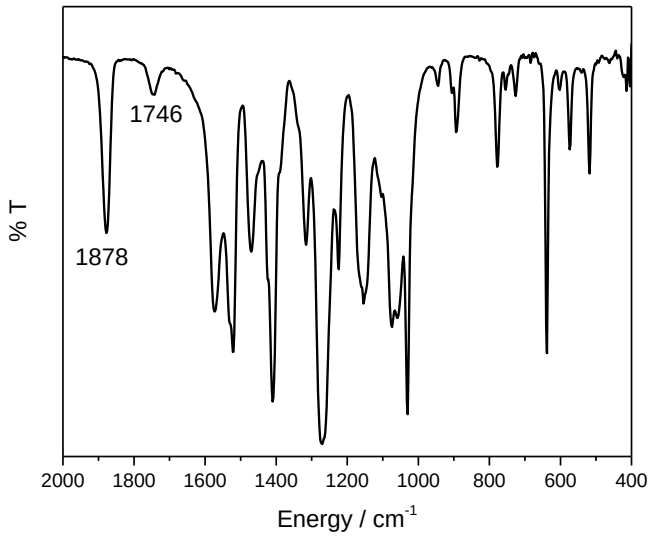

Figure S4. FT-IR spectrum (KBr pellet) of the solid {FeNO}^{6} complex **1** precipitated from an acetonitrile solution with diethyl ether. The band at 1746 cm^{-1} corresponds to a small {FeNO}^{7} impurity.

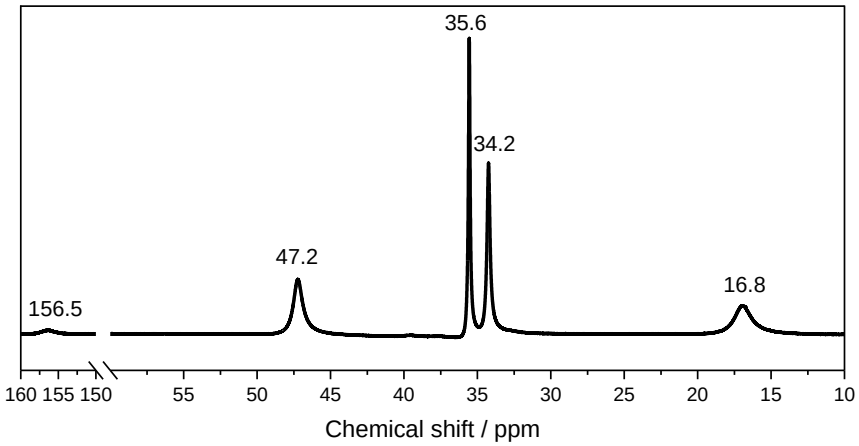

Figure S5. ^{1}H NMR spectrum (500 MHz, CD_3CN) of the $\{FeNO\}^6$ complex **1**.

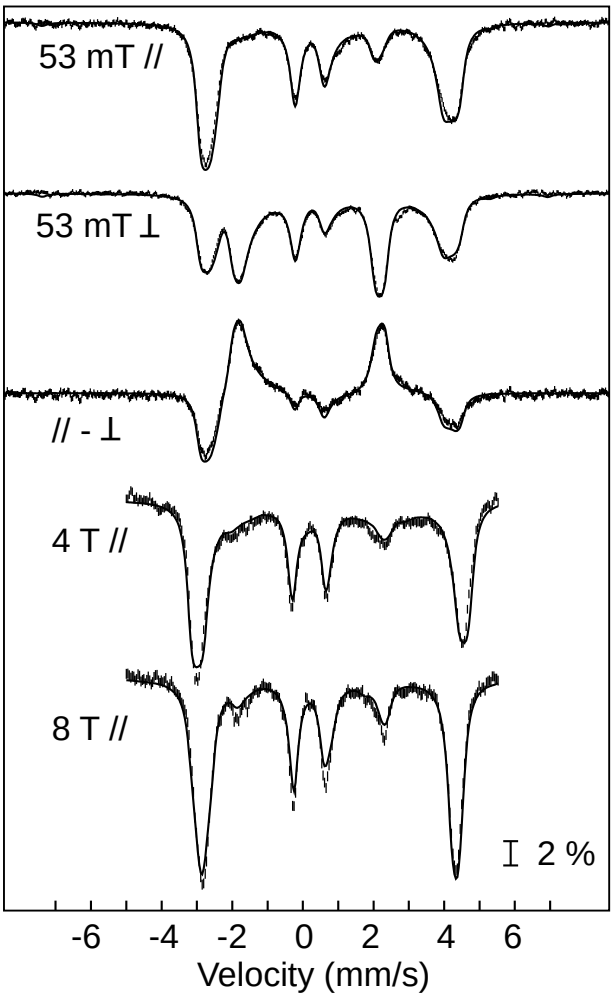

Figure S6. 4.2-K/variable-field (// = parallel, ⊥ = perpendicular magnetic field) Mössbauer spectra of a 5 mM solution of the {^{57}FeNO}^{7} complex **2** in 1:1 propionitrile:butyronitrile (black vertical bars). Spin Hamiltonian simulations carried out with respect to the total spin of the complex, S = 3/2, using the following parameters are overlaid as blue lines: D = 6.0 cm^{-1}, E/D = 0.07 (obtained independently from analysis of the X-band EPR spectrum), **g** = 2.0, δ = 0.48 mm/s, ΔE_Q = -1.42 mm/s, η = 0.08, **A** = (-21.0, -20.4, -30.0) T. These parameters are similar to those observed for other {FeNO}^{7} complexes with S = 3/2 ground state, albeit with a smaller axial zero-field splitting parameter.[6]

[6] a) S. Ye, J. C. Price, E. W. Barr, M. T. Green, J. M. Bollinger, C. Krebs, F. Neese, *J. Am. Chem. Soc.* **2010**, *132*, 4739-4751 b) C. A. Brown, M. A. Pavlosky, T. E. Westre, Y. Zhang, B. Hedman, K. O. Hodgson, E. I. Solomon, *J. Am. Chem. Soc.* **1995**, *117*, 715-732. c) C. D. Brown, M. L. Neidig, M. B. Neibergall, J. D. Lipscomb, E. I. Solomon, *J. Am. Chem. Soc.* **2007**, *129*, 7427-7438. d) D. M. Arciero, J. D. Lipscomb, B. H. Huynh, T. A. Kent, E. Münck, *J. Biol. Chem.* **1983**, *258*, 14981-14991. e) A. R. Diebold, C. D. Brown-Marshall, M. L. Neidig, J. M. Brownlee, G. R. Moran, E. I. Solomon, *J. Am. Chem. Soc.* **2011**, *133*, 18148-18160.f) A. M. Orville, V. J. Chen, A. Kriauciunas, M. R. Harpel, B. G. Fox, E. Munck, J. D. Lipscomb, *Biochemistry* **1992**, *31*, 4602-4612.

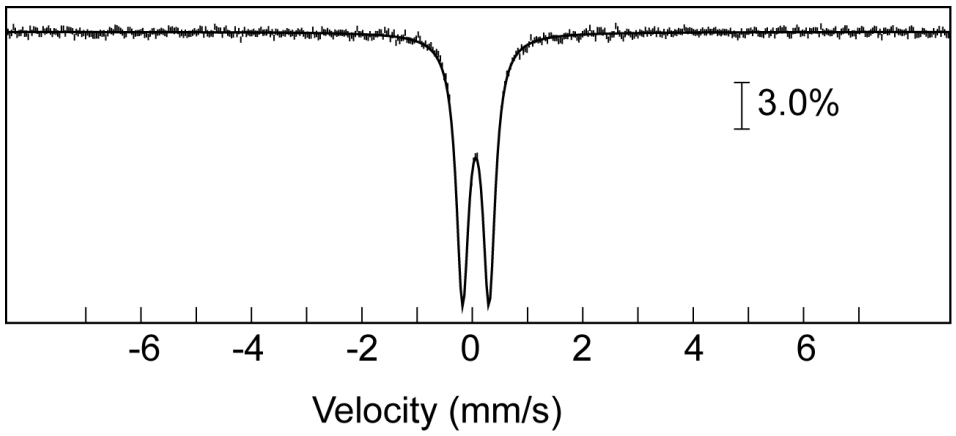

Figure S7. 4.2-K/53-mT parallel field (//) Mössbauer spectrum of a 5 mM solution of the $\{^{57}FeNO\}^6$ complex **2** in 1:1 propionitrile:butyronitrile (black vertical bars) overlaid with a quadrupole doublet simulation using the parameters δ = 0.06 mm/s and $|\Delta E_Q|$ = 0.48 mm/s.

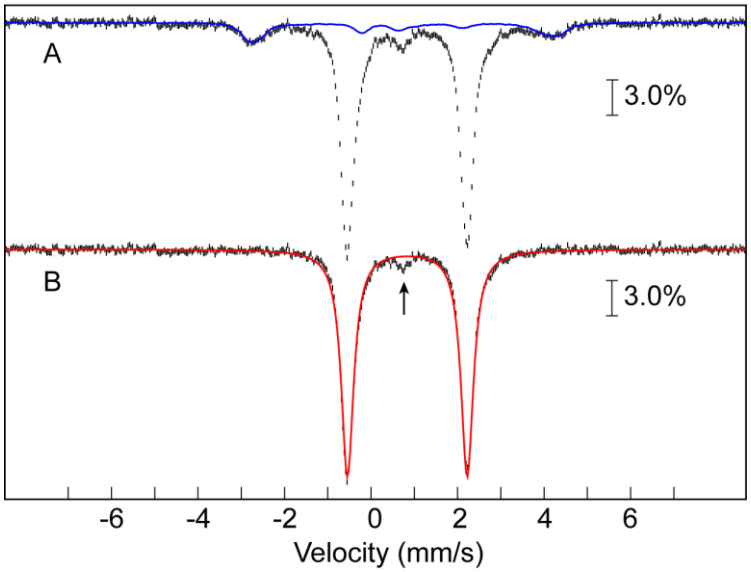

Figure S8. (**A**) 4.2-K/53-mT Mössbauer spectrum of a sample containing 5 mM solution of the $\{^{57}FeNO\}^8$ complex **3** in 1:1 propionitrile:butyronitrile. The magnetic field was applied parallel to the γ–beam. The raw data is shown in vertical bars while the solid blue line is the experimental spectrum of $\{^{57}FeNO\}^7$ complex **1** recorded under identical conditions and scaled to 16% of the total intensity. (**B**) Reference spectrum of the $\{^{57}FeNO\}^8$ complex generated by removal of the contribution from the $\{^{57}FeNO\}^7$ complex. The solid red line is the simulation of the $\{^{57}FeNO\}^8$ complex with δ = 0.84 mm/s and $|\Delta E_Q|$ = 2.78 mm/s. The arrow points at the high-energy line of a small quadrupole doublet (~ 5%), the identity of which remains unclear.

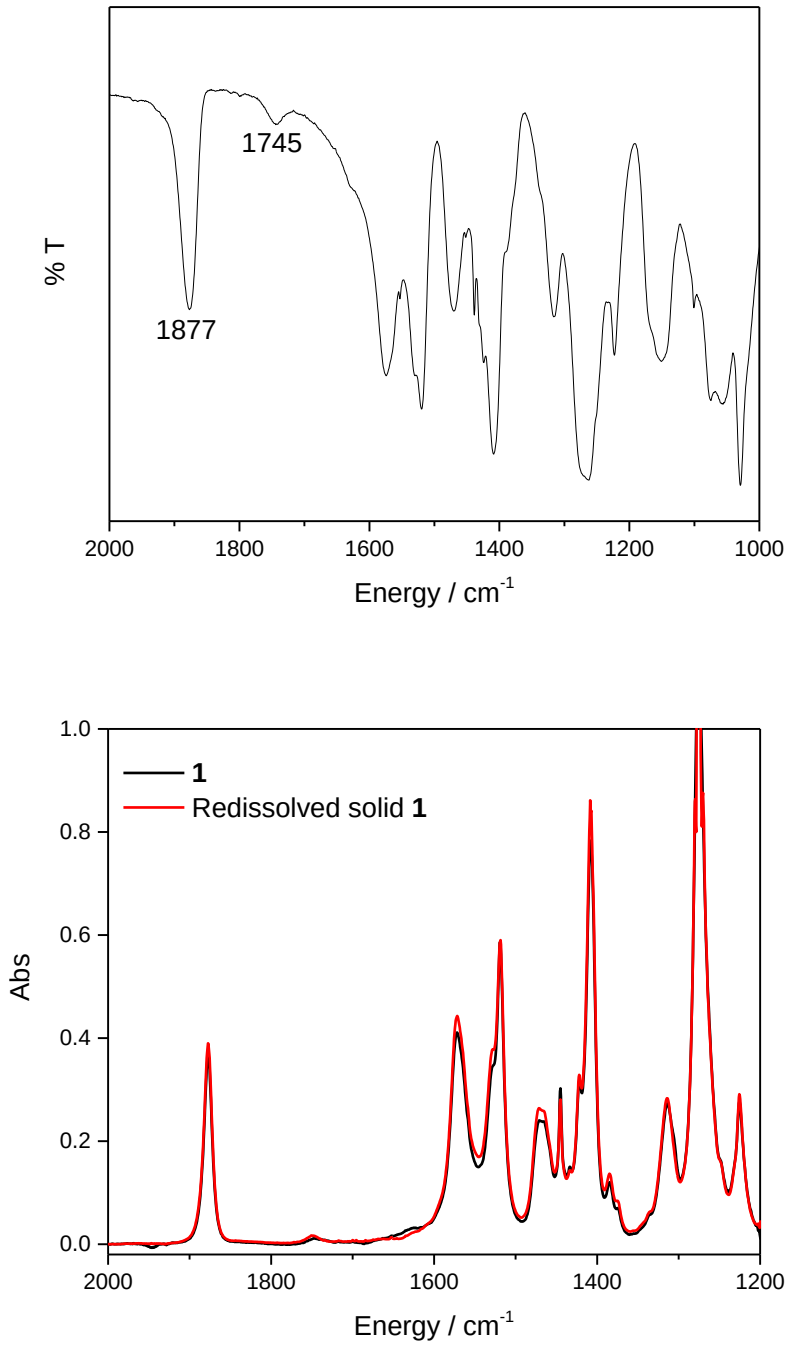

Figure S9. (Top) FT-IR spectrum (KBr pellet) of solid **1** generated in CH_3CN following the removal of solvent under vacuum. (Bottom) Solution IR of the same solid redissolved in CD_3CN (red), which is identical to the solution IR of **1** (black). These data demonstrate that NO remains bound to **1** even under vacuum.

Crystal Structure Determination[7]

At −40°C, 21.4 mg of $[Fe(TMG_3tren)(NO)](BF_4)_2$ (30.6 μmol) and 12.4 mg of thianthrene tetrafluoroborate (40.9 μmol, 1.3 equivalents) were combined in 3 mL of acetonitrile, and the resulting solution was stirred for 10 minutes. Vapor diffusion of diethyl ether into this solution at −35°C gave purple block crystals suitable for x-ray diffraction after 5 days.

A crystal of dimensions 0.26 x 0.18 x 0.16 mm was mounted on a Rigaku AFC10K Saturn 944+ CCD-based X-ray diffractometer equipped with a low temperature device and a Micromax-007HF Cu-target micro-focus rotating anode (λ = 1.54187 A) operated at 1.2 kW power (40 kV, 30 mA). The X-ray intensities were measured at 85(1) K with the detector placed at a distance of 42.00 mm from the crystal. A total of 2028 images were collected with an oscillation width of 1.0° in ω. The exposure times were 1 sec. for the low angle images, 8 sec. for high angle. Rigaku d*trek images were exported to CrysAlisPro for processing and corrected for absorption. The integration of the data yielded a total of 59818 reflections to a maximum 2θ value of 138.80° of which 7340 were independent and 7283 were greater than $2\sigma(I)$. The final cell constants (Table S1) are based on the xyz centroids of 32910 reflections above $10\sigma(I)$. Analysis of the data showed negligible decay during data collection. The structure was solved and refined with the Bruker SHELXTL (version 2014/6) software package, using the space group P2(1)/n with Z = 4 for the formula $C_{25}H_{54}B_3N_{13}OF_{12}Fe$. All non-hydrogen atoms were refined anisotropically with the hydrogen atoms placed in idealized positions. There are two acetonitrile solvate molecules disordered over four sites. Full matrix least-squares refinement based on F^2 converged at R1 = 0.0511 and wR2 = 0.1374 [based on I > 2sigma(I)], R1 = 0.0513 and wR2 = 0.1376 for all data. Additional details are presented in Table S1.

CCDC 1450725 contains the supplementary crystallographic data for this paper. These data can be obtained free of charge from the Cambridge Crystallographic Data Centre via www.ccdc.cam.ac.uk/data_request/cif.

[7] a) Sheldrick, G.M. SHELXTL, v. 2014/6; Bruker Analytical X-ray, Madison, WI, 2014. b) CrystalClear Expert 2.0 r16, Rigaku Americas and Rigaku Corporation (2014), Rigaku Americas, 9009, TX, USA 77381-5209, Rigaku Tokyo, 196-8666, Japan. c) CrysAlisPro 1.171.38.41 (Rigaku Oxford Diffraction, 2015).

Table S1. Crystal data and structure refinement for $[Fe(TMG_3tren)(NO)](BF_4)_3 \bullet 2\ CH_3CN$

Emperical formula	$C_{25}H_{54}B_3F_{12}FeN_{13}O$	
Formula weight	869.09	
Temperature	85(2) K	
Wavelength	1.54178 Å	
Crystal system	Monoclinic	
Space Group	P2(1)/n	
Unit cell dimensions	a = 10.75300(10) Å	α = 90 °
	b = 20.8943(2) Å	β = 90.3620(10) °
	c = 17.60140(10) Å	γ = 90 °
Volume	3954.54(6) $Å^3$	
Z, calculated density	4, 1.460 Mg/m^3	
Absorption coefficient	3.938 mm^{-1}	
F(0,0,0)	1808	
Crystal size	0.260 x 0.180 x 0.160 mm	
Theta range for data collection	3.283° to 69.404°	
Limiting indices	-12<=h<=13, -24<=k<=25, -21<=l<=21	
Reflections collected / unique	59818 / 7340 [R(int) = 0.0563]	
Completeness to theta = 67.679	99.9%	
Absorption correction	Semi-empirical from equivalents	
Max. and min. transmission	1.00000 and 0.50020	
Refinement method	Full-matrix least-squares on F^2	
Data / restraints/parameters	7340 / 474 / 568	
Goodness of fit on F^2	1.095	
Final R indices [I>2sigma(I)]	R1 = 0.0511, wR2 = 0.1374	
R indices (all data)	R1 = 0.0513, wR2 = 0.1376	
Extinction coefficient	0.00142(9)	
Largest diff. peak and hole	1.346 and -0.454 $e.A^{-3}$	

Computational Methods

All geometry optimizations and frequency calculations were performed with the ORCA program package[8] (version 2.9) at the TPSS[9]/def2-TZVP(-f)[10] level employing the RI approximation with the def2-TZV/J auxiliary basis set.[11] The calculated geometric parameters, N-O stretching frequencies, and Mössbauer parameters are in good agreement with experiment (Table S2). The coordinates for the DFT-optimized structures are given in Tables S4-S6. For comparison, the {FeNO}^{6} complex **1** was also optimized in the S = 0 and S = 2 spin states. These structures were 23 kcal/mol and 14 kcal/mol higher in energy, respectively, than the S = 1 structure providing further evidence that **1** has an S = 1 ground state.

Mössbauer parameters were calculated using the B3LYP[12] and TPSS functionals and the basis sets CP(PPP)[13] on Fe, TZVP[10] on N and O, and SV(P)[10] on C and H. Isomer shifts (δ) were calculated using the correlation between $\rho(0)$ (the electron density at the iron nucleus) and δ reported in the literature.[14] For both TPSS and B3LYP, the calculated Mössbauer parameters are in good agreement with experiment (Table S3). More importantly, the trends in δ (and to a lesser degree $|\Delta E_Q|$) are well-reproduced (Figures S10 and S11) for both the {FeNO}$^{6\text{-}8}$ and other TMG_3tren complexes, indicating that DFT is able to properly replicate changes in electronic structure in TMG_3tren compounds.

In order to examine bonding, single-point calculations were performed at the B3LYP/def2-TZVP(-f) level employing the RIJCOSX[15] approximation with the def2-TZV/J auxiliary basis set. To facilitate comparison between the {FeNO}^{6}, {FeNO}^{7}, and {FeNO}^{8} complexes, the canonical orbitals for the broken symmetry solutions were transformed into unrestricted corresponding orbitals (UCOs).[16] Note that because of the underlying transformation, the orbital energies for the UCOs are not well-defined. The orbitals were plotted using the orca_plot tool and visualized using Molekel version 5.4[17] (electron density isosurface value = 0.05).

[8] F. Neese, *Wiley Interdiscip. Rev.: Comput. Mol. Sci.* **2012**, *2*, 73-78.
[9] a) J. Tao, J. P. Perdew, V. N. Staroverov, G. E. Scuseria, *Phys. Rev. Lett.* **2003**, *91*, 146401. b) J. P. Perdew, J. Tao, V. N. Staroverov, G. E. Scuseria, *J. Chem. Phys.* **2004**, *120*, 6898-6911.
[10] a) A. Schäfer, H. Horn, R. Ahlrichs, *J. Chem. Phys.* **1992**, *97*, 2571-2577. b) F. Weigend, R. Ahlrichs, *PCCP* **2005**, *7*, 3297-3305.
[11] a) K. Eichkorn, O. Treutler, H. Öhm, M. Häser, R. Ahlrichs, *Chem. Phys. Lett.* **1995**, *240*, 283-290. b) K. Eichkorn, F. Weigend, O. Treutler, R. Ahlrichs, *Theor. Chem. Acc.* **1997**, *97*, 119-124.
[12] a) A. D. Becke, *J. Chem. Phys.* **1993**, *98*, 5648-5652. b) C. Lee, W. Yang, R. G. Parr, *Phys. Rev. B* **1988**, *37*, 785-789.
[13] F. Neese, *Inorg. Chim. Acta* **2002**, *337*, 181-192.
[14] M. Römelt, S. Ye, F. Neese, *Inorg. Chem.* **2009**, *48*, 784-785.
[15] F. Neese, F. Wennmohs, A. Hansen, U. Becker, *Chem. Phys.* **2009**, *356*, 98-109.
[16] F. Neese, *J. Phys. Chem. Solids* **2004**, *65*, 781-785.
[17] U. Varetto, Molekel 5.4

Table S2. Comparison of DFT-calculated geometric parameters and N-O stretching frequencies to experimental values.

	{FeNO}^{6} Expt.	{FeNO}^{6} DFT	{FeNO}^{7} Expt.	{FeNO}^{7} DFT	{FeNO}^{8} Expt.	{FeNO}^{8} DFT
Fe-N(O) (Å)	1.680	1.666	1.748	1.721	--	1.694
N-O (Å)	1.142	1.151	1.154	1.177	--	1.202
Fe-N-O (°)	180	180	168	154	--	159
Fe-N_{amine} (Å)	2.020	2.042	2.251	2.222	--	2.112
Avg. Fe-N_{guan} (Å)	1.966	2.008	2.037	2.071	--	2.313
ν(NO) (cm^{-1})	1878[a,b]	1874	1730-1740[a,c] 1750[b]	1714	1618[b]	1628

[a] Solid state (KBr pellet) [b] In CD_3CN solution [c] The NO stretch of the {FeNO}^{7} complex **1** in the solid state varies depending on the conditions of isolation. However, regardless of the solid-state NO stretch, all compounds exhibit ν(NO) = 1750 cm^{-1} upon redissolving in CD_3CN solution.

Table S3. Comparison of DFT-calculated Mössbauer parameters to experimental values.

	δ (mm/s)			$\lvert\Delta E_Q\rvert$ (mm/s)		
	Expt.	**B3LYP**	**TPSS**	**Expt.**	**B3LYP**	**TPSS**
{FeNO}^{8} (3)	0.84	0.72	0.81	2.78	2.13	1.62
{FeNO}^{7} (2)	0.48	0.38	0.52	1.42	1.69	1.33
{FeNO}^{6} (1)	0.06	0.07	0.19	0.48	0.40	0.49
Fe(IV)=O[18]	0.09	0.07	0.19	0.29	0.55	0.46
Fe(IV)-CN[19]	-0.19	-0.21	-0.10	4.45	5.25	4.76

[18] J. England, M. Martinho, E. R. Farquhar, J. R. Frisch, E. L. Bominaar, E. Münck, L. Que Jr., *Angew. Chem.* **2009**, *121*, 3676-3680; *Angew. Chem. Int. Ed.* **2009**, *48*, 3622-3626.
[19] J. England, E. R. Farquhar, Y. Guo, M. A. Cranswick, K. Ray, E. Münck, L. Que Jr., *Inorg. Chem.* **2011**, *50*, 2885-2896.

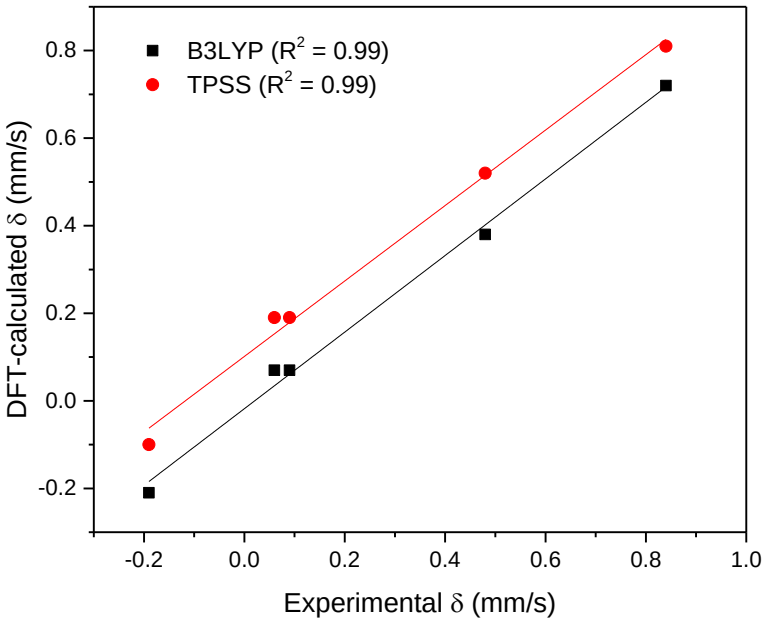

Figure S10. Correlation of experimental and DFT-calculated δ.

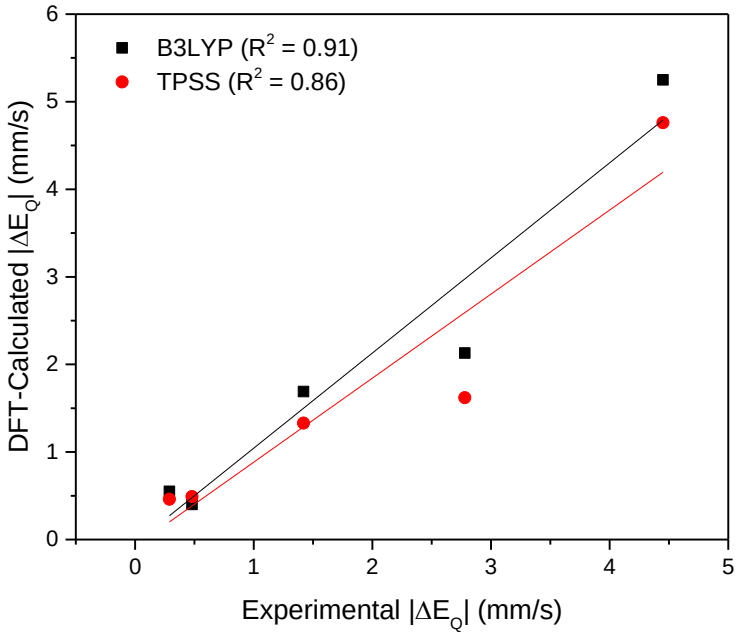

Figure S11. Correlation of experimental and DFT-calculated $|\Delta E_Q|$.

Table S4. Coordinates for the TPSS/def2-TZVP(-f)-optimized structure of the {FeNO}^{6} complex **1**

	X	Y	Z
Fe	0.00593	-0.01618	0.4616
N	0.00751	0.0045	-1.20466
N	0.00433	-0.0409	2.50298
N	1.31575	-1.52234	0.68233
N	-1.95142	-0.4025	0.69334
N	0.65352	1.86694	0.72275
N	3.2011	-2.72979	-0.11445
N	1.19989	-2.78539	-1.31008
N	-3.94804	-1.41725	-0.10065
N	-3.00623	0.36223	-1.27697
N	0.76395	4.11792	-0.03083
N	1.82716	2.436	-1.24657
C	0.59671	-1.34646	2.96762
H	-0.17024	-2.11691	2.87149
H	0.87558	-1.25698	4.02379
C	1.78123	-1.66965	2.08497
H	2.62255	-1.00481	2.30876
H	2.11651	-2.69443	2.27242
C	1.91361	-2.33118	-0.24669
C	4.26321	-1.88374	0.45665
H	3.91829	-0.85495	0.53851
H	5.12433	-1.91767	-0.21747
H	4.57832	-2.25524	1.43693
C	3.65501	-4.08437	-0.50782
H	2.79583	-4.73088	-0.67806
H	4.24623	-4.48871	0.31867
H	4.28356	-4.04726	-1.40225
C	1.827	-3.09416	-2.60996
H	2.81063	-2.62962	-2.66639
H	1.18924	-2.68241	-3.39836
H	1.91761	-4.17288	-2.77005
C	-0.19844	-3.21926	-1.18592
H	-0.54751	-3.01176	-0.17643
H	-0.26007	-4.29519	-1.3842
H	-0.82741	-2.70087	-1.91676
C	-1.41821	0.08988	2.98314
H	-1.70297	1.1408	2.90863
H	-1.47049	-0.2156	4.03445
C	-2.29832	-0.75819	2.09294
H	-2.1407	-1.82315	2.29533

H	-3.35169	-0.54032	2.29448
C	-2.95981	-0.49999	-0.2277
C	-3.74193	-2.76891	0.44759
H	-2.67792	-2.98662	0.51564
H	-4.2091	-3.48685	-0.23317
H	-4.21165	-2.87099	1.43108
C	-5.35176	-1.1262	-0.47565
H	-5.48277	-0.05644	-0.62928
H	-5.98946	-1.44736	0.35278
H	-5.64341	-1.67603	-1.37515
C	-3.60216	-0.00498	-2.57641
H	-3.69328	-1.08799	-2.6493
H	-2.93533	0.35369	-3.36664
H	-4.58303	0.45906	-2.71795
C	-2.67937	1.78758	-1.13364
C	0.83304	1.11647	2.99779
H	1.8848	0.83908	2.90951
H	0.60333	1.29502	4.0545
C	0.53116	2.31898	2.13224
H	-0.46813	2.71102	2.35064
H	1.24834	3.11846	2.34249
C	1.06485	2.80642	-0.18444
C	-0.50659	4.60341	0.53482
H	-1.22567	3.78873	0.59284
H	-0.90028	5.37869	-0.12932
H	-0.35412	5.04346	1.52548
C	1.71411	5.19607	-0.39218
H	2.70576	4.779	-0.55894
H	1.75858	5.894	0.44866
H	1.37783	5.73905	-1.28016
C	1.7955	3.15864	-2.53314
H	0.9014	3.7784	-2.58795
H	1.76782	2.41592	-3.33653
H	2.68547	3.78027	-2.67072
C	2.90075	1.4396	-1.12967
H	2.88386	1.01351	-0.12862
H	3.8655	1.92797	-1.30701
H	2.77499	0.65048	-1.87794
O	0.00867	0.01919	-2.35598
H	-1.92403	2.08379	-1.86859
H	-2.31318	1.96956	-0.12529
H	-3.58169	2.38317	-1.31204

Table S5. Coordinates for the TPSS/def2-TZVP(-f)-optimized structure of the {FeNO}^{7} complex **2**

	X	Y	Z
Fe	-0.02639	-0.01152	0.29165
N	-0.02659	0.03476	-1.42904
N	-0.03116	-0.05652	2.51271
N	1.25883	-1.63939	0.63271
N	-2.04717	-0.3005	0.63405
N	0.75221	1.84347	0.64336
N	3.04822	-3.03278	-0.10575
N	1.05266	-2.95527	-1.29866
N	-4.13038	-1.15111	-0.14433
N	-3.13108	0.65805	-1.21433
N	1.12975	4.08845	-0.05091
N	2.16564	2.33513	-1.17179
C	0.59091	-1.33933	2.94877
H	-0.17133	-2.11985	2.88336
H	0.92244	-1.2721	3.99376
C	1.7501	-1.68677	2.02424
H	2.57495	-0.98029	2.18615
H	2.12825	-2.68363	2.27659
C	1.78821	-2.51707	-0.23528
C	4.17985	-2.25699	0.41397
H	3.91759	-1.20151	0.45283
H	5.02984	-2.38299	-0.26492
H	4.48054	-2.59837	1.41079
C	3.36857	-4.42781	-0.45358
H	2.44926	-4.98649	-0.62456
H	3.90349	-4.87825	0.38869
H	4.00661	-4.48621	-1.34198
C	1.65643	-3.28913	-2.59514
H	2.68901	-2.9428	-2.6216
H	1.09077	-2.78014	-3.38296
H	1.62818	-4.36675	-2.79121
C	-0.39051	-3.17566	-1.21062
H	-0.71557	-2.96536	-0.1929
H	-0.61168	-4.21992	-1.46301
H	-0.93073	-2.5262	-1.90731
C	-1.44994	0.03451	2.96185
H	-1.74715	1.08584	2.93397
H	-1.55242	-0.32277	3.99537
C	-2.32804	-0.76504	2.01071
H	-2.12068	-1.83661	2.12556

H	-3.38164	-0.61064	2.26766
C	-3.08363	-0.27948	-0.22539
C	-3.97337	-2.54478	0.28801
H	-2.91846	-2.81235	0.29033
H	-4.49992	-3.19025	-0.42251
H	-4.39838	-2.7082	1.28455
C	-5.51632	-0.75339	-0.44843
H	-5.57774	0.32982	-0.54393
H	-6.15469	-1.07129	0.38198
H	-5.87842	-1.22681	-1.36711
C	-3.73285	0.3963	-2.52899
H	-3.91095	-0.6721	-2.64636
H	-3.03077	0.72652	-3.30157
H	-4.67434	0.94091	-2.66019
C	-2.65964	2.02846	-1.00678
C	0.7594	1.12146	2.96758
H	1.81867	0.85599	2.92507
H	0.51236	1.3787	4.00648
C	0.49184	2.29165	2.03273
H	-0.5425	2.63737	2.15451
H	1.14599	3.12894	2.29742
C	1.32538	2.74373	-0.18289
C	-0.14986	4.6688	0.37279
H	-0.92567	3.90632	0.34745
H	-0.41786	5.46896	-0.32496
H	-0.08382	5.09553	1.37976
C	2.20187	5.07103	-0.28928
H	3.15918	4.55924	-0.37863
H	2.24203	5.74873	0.56943
H	2.01357	5.66286	-1.19119
C	2.29007	3.04606	-2.45296
H	1.48776	3.77614	-2.54942
H	2.20196	2.31472	-3.26248
H	3.25857	3.54977	-2.54105
C	3.02502	1.15994	-1.02999
H	2.9265	0.77102	-0.01803
H	4.06431	1.45401	-1.2175
H	2.74939	0.38178	-1.74971
O	-0.0499	0.58054	-2.47106
H	-1.83952	2.26875	-1.6907
H	-2.32328	2.13108	0.02385
H	-3.48538	2.7247	-1.19648

Table S6. Coordinates for the TPSS/def2-TZVP(-f)-optimized structure of the {FeNO}^{8} complex **3**

	X	Y	Z
Fe	-0.01251	-0.08646	0.13172
N	-0.08741	0.0609	-1.55431
O	-0.41508	0.48916	-2.62863
N	0.0429	-0.12186	2.49035
N	1.95052	-0.95566	0.62122
N	-1.80242	-1.15491	0.64859
N	-0.16072	1.98342	0.61446
N	4.18369	-1.39944	-0.10138
N	2.3719	-2.31572	-1.23628
N	-3.34887	-2.82148	-0.08198
N	-3.34099	-0.7088	-1.06115
N	-0.73351	4.22776	0.04459
N	0.92913	3.11086	-1.13905
C	1.2205	-0.91003	2.92639
H	0.94971	-1.96911	2.87857
H	1.49081	-0.67543	3.9682
C	2.39716	-0.6605	1.98683
H	2.72766	0.38337	2.08682
H	3.24124	-1.29536	2.2871
C	2.81148	-1.52003	-0.2074
C	4.8266	-0.15893	0.32705
H	4.09287	0.64488	0.34789
H	5.61231	0.104	-0.3918
H	5.28623	-0.25548	1.31893
C	5.09736	-2.49795	-0.42514
H	4.5254	-3.41118	-0.58772
H	5.78371	-2.65315	0.41585
H	5.69447	-2.28139	-1.32045
C	2.96568	-2.25821	-2.57376
H	3.79805	-1.55494	-2.57709
H	2.21232	-1.91422	-3.29314
H	3.3258	-3.24474	-2.88975
C	1.1165	-3.05353	-1.14319
H	0.83034	-3.1224	-0.09334
H	1.26974	-4.06087	-1.55037
H	0.31273	-2.56003	-1.70066
C	-1.22316	-0.7404	2.95821
H	-1.98549	0.04153	3.00976
H	-1.10383	-1.16483	3.96686

C	-1.67533	-1.80209	1.96313
H	-0.93788	-2.61824	1.94447
H	-2.6284	-2.23527	2.29211
C	-2.78622	-1.55978	-0.14015
C	-2.54505	-4.01599	0.16271
H	-1.4886	-3.76576	0.07521
H	-2.789	-4.77373	-0.5921
H	-2.73378	-4.44646	1.15487
C	-4.78257	-3.05185	-0.27241
H	-5.30138	-2.09435	-0.31492
H	-5.17198	-3.62922	0.57497
H	-4.98596	-3.61343	-1.19347
C	-3.72477	-1.15143	-2.40408
H	-3.52946	-2.21851	-2.50823
H	-3.13034	-0.61005	-3.14907
H	-4.78791	-0.95959	-2.59395
C	-3.33271	0.73574	-0.85489
C	0.13939	1.29328	2.92174
H	1.19001	1.59327	2.87676
H	-0.2028	1.41162	3.96206
C	-0.66708	2.18056	1.979
H	-1.7314	1.91437	2.04714
H	-0.56907	3.2255	2.29852
C	-0.00473	3.064	-0.1344
C	-2.15296	4.21349	0.38633
H	-2.53413	3.19653	0.31111
H	-2.70211	4.84771	-0.32116
H	-2.33612	4.59312	1.40027
C	-0.13571	5.55612	-0.10197
H	0.94135	5.4577	-0.23662
H	-0.32762	6.14268	0.80514
H	-0.55717	6.09962	-0.9577
C	0.66821	3.77117	-2.42007
H	-0.33522	4.19561	-2.4166
H	0.73343	3.03337	-3.22803
H	1.39722	4.56892	-2.609
C	2.14992	2.31793	-1.08285
H	2.24506	1.89679	-0.08282
H	3.00818	2.96631	-1.30391
H	2.12917	1.49773	-1.80915
H	-2.56299	1.22598	-1.45987
H	-3.14257	0.93385	0.1996
H	-4.31467	1.13615	-1.13646